Phonon-generated microfields and temperature dependence of the absorption edge in II-VI compounds*

B. G. Yacobi, Y. Brada, U. Lachish, and C. Hirsch
The Racah Institute of Physics, The Hebrew University, Jerusalem, Israel
(Received 13 March 1974; revised manuscript received 16 December 1974)

The strong temperature dependence of the exponential absorption edges in three structures of ZnS has been measured between 10 and 300 °K. The Dow-Redfield theory of phonon-generated microfields and their influence on the absorption edge through a Franz-Keldysh mechanism are used to explain the results. Below 50 °K only a very slight change in the edge energy E_g was observed. Between 55 and 100 °K the energy of the edge could be described by $E_g(T) = E_{g1}(0) - S_1[1 - \tanh(\hbar\omega_{LA}/2kT)]$ and between 100 and 300 °K the edge changed as $E_g(T) = E_{g2}(0) - S_2[1 - \tanh(\hbar\omega_{LO}/2kT)]$, where $\hbar\omega_{LA} = 13.6$ meV, $\hbar\omega_{LO} = 43.5$ meV, and $E_{g1}(0)$, $E_{g2}(0)$, S_1 and S_2 are specific constants of each ZnS structure. The experimental values of the LO-phonon-generated rms field $(\langle F_{LO}^2 \rangle)^{1/2}$ at room temperature were found (in units of 10^5 V/cm) to be 3.90 in the cubic case, 4.77 ($\vec{E} \perp \vec{C}$) and 5.20 ($\vec{E} \parallel \vec{C}$) in the 4*H* polytype, and 6.34 ($\vec{E} \perp \vec{C}$) and 7.62 ($\vec{E} \parallel \vec{C}$) in the hexagonal structure of ZnS. The applicability of the postulated model of the temperature shift of the absorption edge was checked also on known data pertaining to hexagonal CdS. The experimental values of the $(\langle F_{LO}^2 \rangle)^{1/2}$ (in units of 10^5 V/cm) were found to be 3.97 ($\vec{E} \perp \vec{C}$) and 5.90 ($\vec{E} \parallel \vec{C}$).

INTRODUCTION

ZnS is known to crystallize in cubic, hexagonal, and a great number of polytypic forms.[1] An optically significant structure parameter of the polytypes is the percentage of hexagonality β, which is 0 for the cubic crystal, 100 for the hexagonal crystal, and 50 for the 4*H* modification.[2] Both the birefringence and the absorption-edge energy depend linearly on this parameter.[2]

ZnS crystals are known to have an exponential absorption edge,[3,4] which can be represented by the Urbach rule[5]

$$\alpha = \alpha_0 \exp[\sigma(h\nu - h\nu_0)/kT], \quad (1)$$

where α is the absorption coefficient; h, ν, k, and T have the usual meaning; and α_0, σ, and ν_0 are constants of the material. This exponential shape of the absorption coefficient was found to hold also in CdS.[6] The slope parameter σ in some ionic crystals was found to depend on a phonon energy[7]

$$\sigma = \sigma_0(2kT/\hbar\omega_0)\tanh(\hbar\omega_0/2kT), \quad (2)$$

where $\hbar\omega_0$ was defined as an "effective" phonon energy and is again a specific parameter of the material. In some covalent crystals the slope parameter σ was found to depend on the concentrations and the electrical charges of the impurities.[8,9]

The problem of the temperature dependence of the absorption edge in semiconductors and insulators has been approached from several points of view.[10-12] In general there are two main reasons for the temperature dependence of the absorption edge in any semiconductor or insulator. First the band structure must be a function of the crystal-lattice spacing, so that the lattice dilatation may be expected to contribute to a change in the absorption-edge energy. The second contribution is due to the electron-phonon interactions.

In CdS and ZnS, Hohler[13] and Piper *et al.*[14] have shown that the dilatation effect can contribute at most 20% to a change in the absorption-edge energy. From data on the pressure dependence of the edge energy, the elastic constants, and the thermal-expansion coefficients, we deduce that in cubic ZnS this would amount to only 10%.

Möglich *et al.*[10] attempted to explain the temperature dependence of the absorption edge by suggesting that the lattice vibrations cause a temperature-dependent broadening of the energy levels. However, their calculations predicted too small an effect to explain the experimental results in CdS.[13] Later, Radkowski[11] and Fan[12] considered the broadening of energy levels due to polar modes of vibrations[11] and the shift of these levels as associated with the electron-phonon coupling.[12]

Piper *et al.*[14,15] tried to fit the observed temperature shift of the ZnS absorption edge to Fan's theory.[12] However, too high an effective mass of $m^* = 3.3m_0$ (m_0 is the free-electron mass) had to be introduced for both electrons and holes.

The temperature dependence of the energy gap of the direct Γ-point transition in cubic ZnS has been recently computed by a band-theoretical method involving pseudopotentials and the Debye-Waller factor.[16] These results were adjusted for available experimental data.

Also recently, Dow and Redfield[17] presented a unified model pertaining both to the exponential form of the absorption edges and their temperature dependence. This theory applies both to ionic and covalent materials and is essentially based on two previous models: Redfield's internal Franz-Keldysh mechanism[18] and Dexter's Stark-shifted exciton model.[19] This unified theory explains the exponential edges as being due to the field ionization of the exciton, i.e., the field-induced tunnelling of the electron away from the hole. The dominant sources of the ionizing electric microfields may be charged imperfections such as phonons, impurities, and dislocations. As ZnS possesses both polar and piezoelectric phonons, these certainly could affect both the form and the energy value of the absorption edge.

The mean-square field $\langle F^2\rangle$ of LO phonons has been evaluated by Dow and Redfield[17] from the polaron theory[20] assuming a Gaussian distribution of fields and was found to be

$$\langle F^2\rangle = \frac{\hbar\omega_{LO} q_c^3(\epsilon_0 - \epsilon_\infty)}{3\pi\epsilon_0\epsilon_\infty}\coth\left(\frac{\hbar\omega_{LO}}{2kT}\right), \tag{3}$$

where $\hbar$, ω, k, and T have the usual meaning; q_c is the polaron cutoff wave vector, normally of the order of π/a, where a is the exciton radius; ϵ_0 and ϵ_∞ are the static and optical dielectric constants, respectively.

As the theory is based on the assumption of a quasiuniform field in the vicinity of the exciton, only such phonons whose wavelength is larger than a, the exciton radius, have to be considered. In this case the wave vector q_c of the active LO phonons has to satisfy the relation $q_c \leq \pi/a$. In strongly ionic materials with a small exciton radius, a can be as small as the lattice constant.

In the present work we will combine the Dow-Redfield model[17] with the Franz-Keldysh theory[21] pertaining to electric-field-induced shifts of exponential absorption edges.

Franz,[21] in the weak-field approximation, obtained

$$\Delta E_g = -[\sigma^2\hbar^2 e^2/24\mu^*(kT)^2]F^2 = -\gamma F^2 , \tag{4}$$

where ΔE_g is the shift of the absorption edge, F is the applied electric field, μ^* is the reduced exciton mass, γ is the Franz-Keldysh coefficient (FKC), and the other symbols have the previous meanings.

We can now connect the Franz-Keldysh effect with the temperature shift of the absorption edge by introducing Eq. (3) into Eq. (4) and by substituting $\langle F^2\rangle$ for F^2. σ/kT can also be introduced from Eq. (2), if we assume that one type of phonons (in this case the LO phonons) are responsible for the absorption-edge phenomena for all electron-phonon interactions. Then, we obtain

$$\Delta E_g = E_g(T_1) - E_g(T_2) = S\left[\tanh\left(\frac{\hbar\omega_{LO}}{2kT_1}\right) - \tanh\left(\frac{\hbar\omega_{LO}}{2kT_2}\right)\right], \tag{5}$$

where

$$S = [e^2\hbar\sigma_0^2 q_c^3(\epsilon_0 - \epsilon_\infty)]/(18\pi\omega_{LO}\epsilon_0\epsilon_\infty\mu^*) \tag{6}$$

and $T_2 > T_1$.

At the lower temperatures, when $T_1 < 100$ °K the first term in the brackets will be almost unity. At these lower temperatures other types of phonons such as piezoelectric acoustic phonons can provide the electrical field. So for example, below 100 °K, the piezoelectric LA phonons in the ⟨111⟩ direction in the cubic case will have the major influence.[22] As is shown in the appendix, the expected temperature dependence of the $\langle F^2\rangle$ due to these phonons has the form

$$\langle F^2\rangle \propto \coth(\hbar\omega_c/2kT), \tag{7}$$

where ω_c is the frequency associated with the polaron cutoff wave vector q_c and not necessarily with the zone-boundary values.

It is worthwhile to emphasize, that for ZnS, relations (4)–(6) hold for low temperatures only as long as the LO-phonon-created field does not exceed about 8×10^5 V/cm, i.e., up to room temperature. For higher temperatures a linear relationship between the change in temperature and the shift of the absorption edge has been observed.[23]

EXPERIMENTAL

ZnS platelets, vapor grown in an H_2S atmosphere[1] were used in these experiments. Homogeneous parts were chosen under a polarizing microscope and their structure was ascertained by birefringence measurements. Cubic $3C$, hexagonal $2H$, and polytypic $4H$ structures can be chosen unambiguously by this method. Their thickness ranged between 7 and 98 μm. The crystals were mounted on a thin copper plate in such a manner that the chosen uniform regions were mounted over a corresponding opening in the copper plate. This assembly was fastened to the cold finger of an optical Dewar. All the optics were of fused silica. Another similar opening in a second plate served as reference for the absorption measurements. The experimental arrangement is shown in Fig. 1. The specimen was illuminated by the filtered and polarized light of a 500-W dc xenon lamp through a Jarrell-Ash 0.5-m monochromator with a bandpass of either 0.8 or 1.2 Å.

A fused silica window photomultiplier (EMI 6256S) was used to detect the transmitted light. The resulting signal was amplified, recorded, and

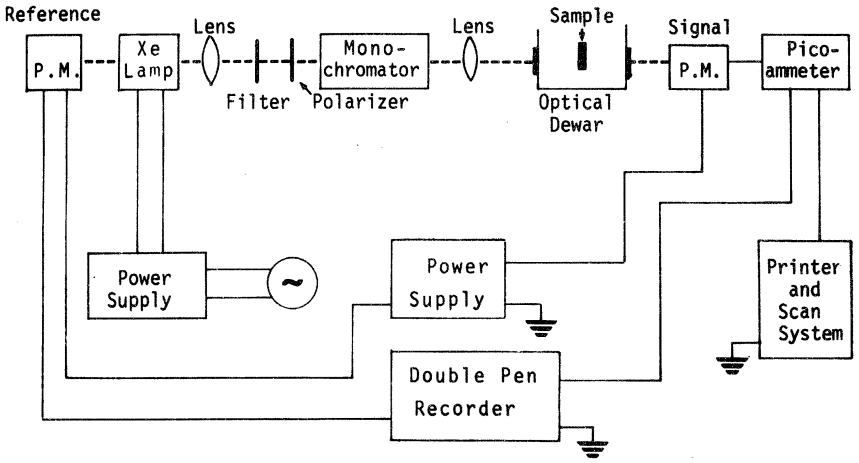

FIG. 1. Experimental arrangement.

digitalized. The total uv emission of the 500-W dc xenon lamp light source was also constantly monitored by a second photomultiplier. The temperatures between 80 and 300 °K were measured by a chromel-alumel thermocouple. For lower temperatures either the boiling points of gases (He, H_2, N_2) or the N_2 triple point were used as reference values. The influence of the optical reflection of the crystal was accounted for by taking the transmission as 100% at 3500 Å, where no significant absorption is observed in our thin samples.

RESULTS AND DISCUSSION

Figure 2 shows the temperature dependence of the absorption edge in cubic (3C) ZnS at 5% transmission, which corresponds in this crystal of 29-μm thickness to an absorption coefficient $\alpha \cong 10^3$ cm^{-1}. Figures 3 and 4 show the temperature dependence of the absorption edge in polytype 4*H* and hexagonal 2*H* structures for both parallel ($\vec{E} \| \vec{C}$) and perpendicular ($\vec{E} \perp \vec{C}$) directions of the electric vector of the polarized light. Again the absorption edges were taken at 5% transmission, which for the 4*H* crystal of 40-μm thickness corresponds to an absorption coefficient $\alpha \cong 7.5 \times 10^2$ cm^{-1}, and for the 2*H* crystal of 7-μm thickness to $\alpha \cong 4 \times 10^3$ cm^{-1}.

From the behavior of the slope parameter σ with temperature[22] we know that below 100 °K a LA phonon of energy $\hbar\omega_{LA} = 13.6$ meV is responsible for the measured changes in σ in agreement with Eq. (2). In order to check the postulated dependence of the absorption edge E_g on the phonon-created fields [Eq. (5)], we drew Figs. 5–7, where the values of E_g at different temperatures are shown against $\tanh(\hbar\omega_{LA}/2kT)$ in three ZnS structures. The straight lines obtained there for

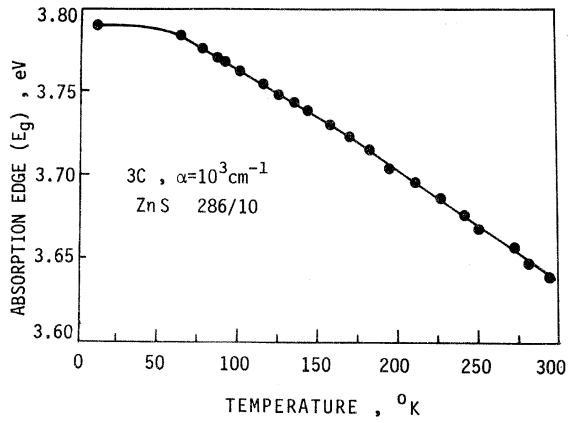

FIG. 2. Temperature dependence of the absorption edge in a cubic (3C) crystal at 5% transmission. Crystal thickness 29 μm.

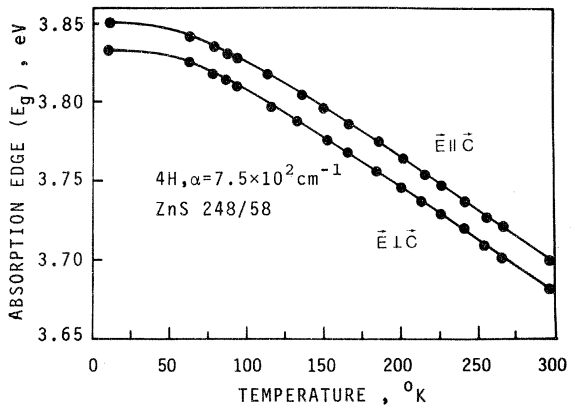

FIG. 3. Temperature dependence of the absorption edge in a polytypic 4*H* crystal at 5% transmission for both perpendicular ($\vec{E} \perp \vec{C}$) and parallel ($\vec{E} \| \vec{C}$) directions of the electric vector $\vec{E}$ of the polarized light. Crystal thickness 40 μm.

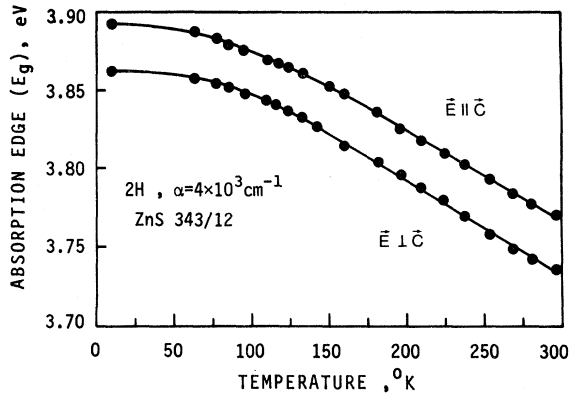

FIG. 4. Temperature dependence of the absorption edge in a hexagonal ($2H$) crystal at 5% transmission for both perpendicular ($\vec{E} \perp \vec{C}$) and parallel ($\vec{E} \parallel \vec{C}$) directions of the electric vector $\vec{E}$ of the polarized light. Crystal thickness 7 μm.

$50 < T < 100$ °K support the view that the electric fields associated with these LA phonons are responsible for most of the temperature shift of the absorption edge in ZnS crystals at these temperatures.

At temperatures above 100 °K the interacting fields are due to the LO phonons.[22] This has been observed both in the behavior of σ with temperature[22] and can be also seen from Figs. 8–10 which correlate the change in the edge energy E_g with $\tanh(\hbar\omega_{LO}/2kT)$. The straight lines obtained between 100 and 300 °K show that the expected behavior of Eq. (5) really holds in this temperature range.

Table I sums up both the experimental results obtained from these graphs and some additional

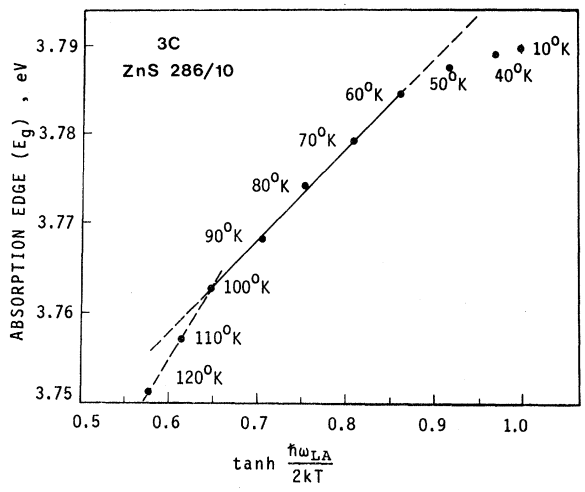

FIG. 5. Absorption edge E_g of cubic ZnS vs $\tanh(\hbar\omega_{LA}/2kT)$.

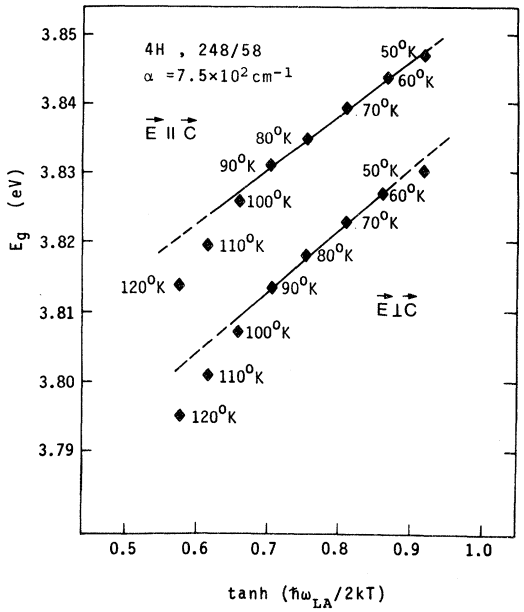

FIG. 6. Absorption edge E_g of $4H$ polytypic ZnS vs $\tanh(\hbar\omega_{LA}/2kT)$.

available data. The LO-phonon energies have been measured by various authors in several ZnS structures. Brafman and Mitra[24] found the same $\hbar\omega_{LO} = 43.5$ meV for both hexagonal and cubic structures. Nilsen measured for the cubic structure[25] $\hbar\omega_{LO} = 43.6$ and 43.1 meV for the hexagonal

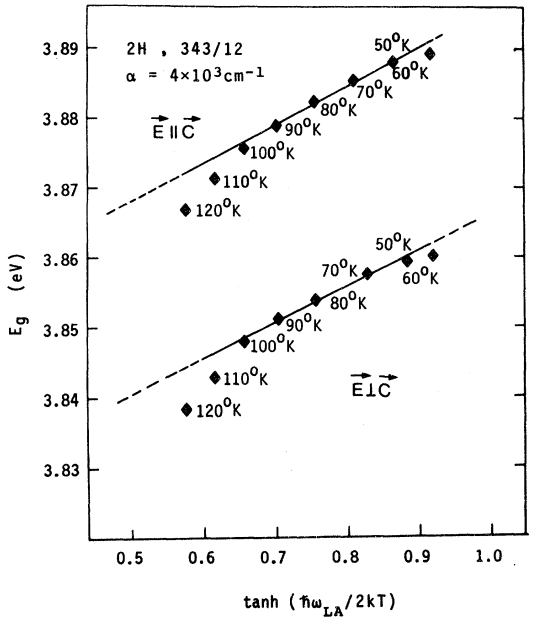

FIG. 7. Absorption edge E_g of hexagonal ZnS vs $\tanh(\hbar\omega_{LA}/2kT)$.

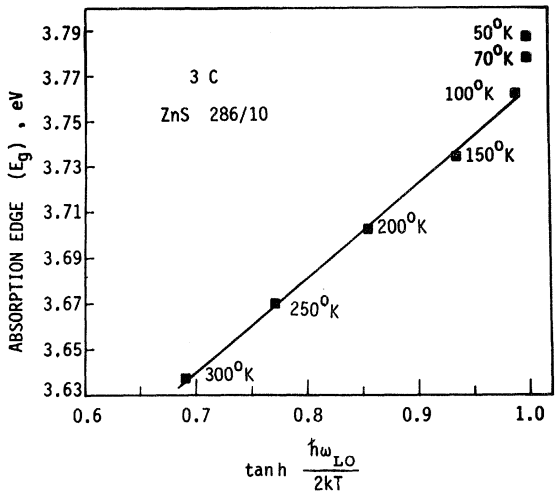

FIG. 8. Absorption edge E_g of cubic ZnS vs $\tanh(\hbar\omega_{LO}/2kT)$.

case.[26] Schneider and Kirby[27] reported for the hexagonal $2H$ and $4H$ polytype structures the LO-phonon energies of 43.1 and 43.3 meV, respectively. The values of ϵ_0 and ϵ_∞ can be found in the literature for the $3C$ structure.[28] For the $2H$ structure we use the $\epsilon_0 = 8.7$ as obtained by Kobyakov and Pado.[29] The value of ϵ_∞ is then computed by the Lyddane-Sachs-Teller relationship.[30] In ZnS polytypes such collective crystal properties as the birefringence and the absorption edge are linear functions of the percentage of hexagonality[2] and thus it seemed justified to use linear interpolation to obtain the values of ϵ_0 and ϵ_∞ for the $4H$ polytype. The dimensions of the exciton radii a have been computed using the previously measured values[31] of the reduced effective exciton masses μ^* and the optical dielectric constants. As the slopes of E_g vs $\tanh(\hbar\omega_{LO}/2kT)$ in Figs. 8–10 contain q_c as the only unknown parameter, one can compute q_c from the experimental results. Table I compares the measures values of q_c against π/a and $\pi/2a$, where the exciton radii have been computed as mentioned above. The table shows that $q_c \lesssim \pi/a$, fully supporting the contention by Dow and Redfield, that $\pi/2a \leq q_c \leq \pi/a$, as they expected from the requirement of a quasiconstant field around the hole-electron pair.

We can also compare the theoretical values of $(\langle F^2\rangle)^{1/2}$ with the experimental values computed from the temperature shift of the absorption edge and the known values of the FKC: $\gamma = -\Delta E_g/F^2$ for

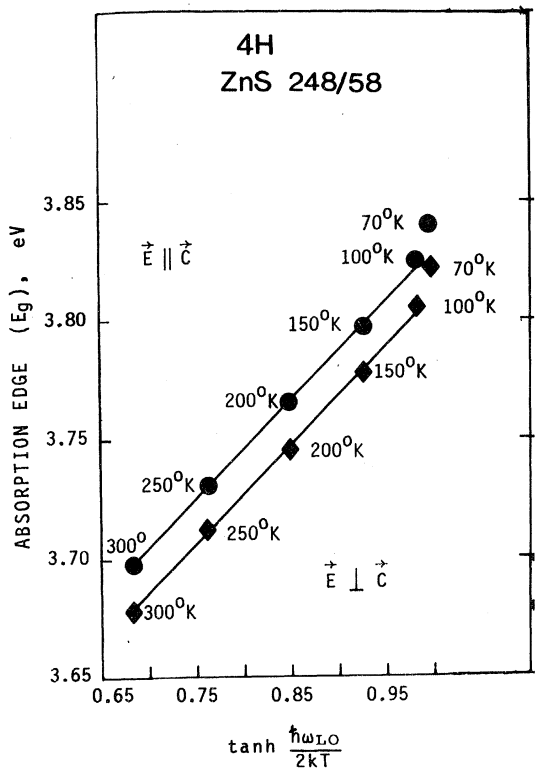

FIG. 9. Absorption edge E_g of $4H$ polytypic ZnS vs $\tanh(\hbar\omega_{LO}/2kT)$.

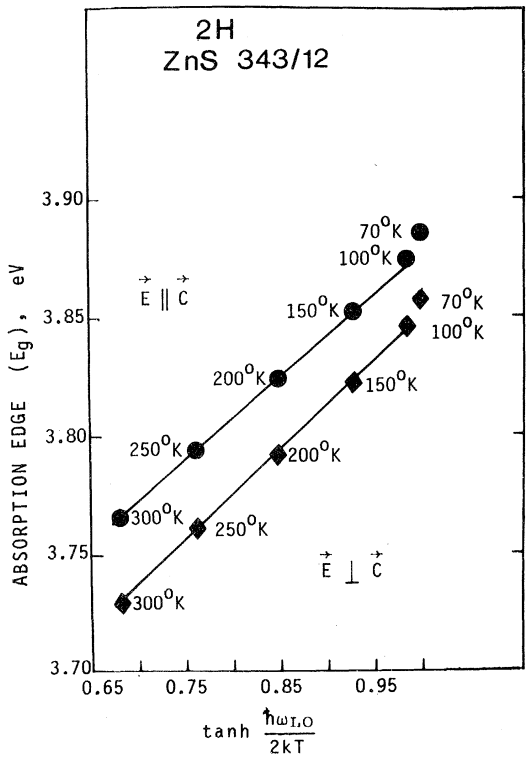

FIG. 10. Absorption edge E_g of hexagonal ZnS vs $\tanh(\hbar\omega_{LO}/2kT)$.

TABLE I. ZnS; static (ϵ_0) and optical (ϵ_∞) dielectric constants; reduced effective exciton mass μ^* (in units of m_0); the 1s exciton radius $a = \hbar^2\epsilon_\infty/\mu^* e^2$; the slope parameter constant σ_0; the parameter S_{LA} from Figs. 5–7; the parameter S_{LO} from Figs. 8–10; the polaron cutoff wave vector q_c from the experimental results [Eq. (6)].

ZnS structure	Polarization of light	ϵ_0	ϵ_∞	μ^* (m_0)	a (Å)	σ_0	S_{LA} (eV)	S_{LO} (eV)	q_c (expt) (10^{-7} cm^{-1})	π/a (10^{-7} cm^{-1})	$\pi/2a$ (10^{-7} cm^{-1})
3C		8.3 [a]	5.1 [a]	0.12 [b]	22.5	2.5	0.106	0.460	1.33	1.40	0.70
4H	$\vec{E}\perp\vec{C}$	8.5	5.2	0.17 [b]	16.2	2.6	0.082	0.414	1.47	1.94	0.97
	$\vec{E}\parallel\vec{C}$			0.19 [b]	14.5	2.5	0.078	0.400	1.54	2.17	1.09
2H	$\vec{E}\perp\vec{C}$	8.7 [c]	5.3	0.22 [b]	12.8	2.5	0.057	0.372	1.58	2.45	1.23
	$\vec{E}\parallel\vec{C}$			0.26 [b]	11.0	2.6	0.052	0.346	1.60	2.86	1.43

[a] Reference 28.
[b] Reference 31.
[c] Reference 29.

the cubic 3C, hexagonal 2H and 4H polytype structures, which have been measured previously.[31] All this is done under the assumption that the measured shift of the absorption edge is due only to the phonon-created electric fields.

For the LO-phonon case,

$$E_g(100\ ^\circ\mathrm{K}) = E_{g0} - \gamma_{100}\langle F_{100}^2\rangle \tag{8}$$

and

$$E_g(300\ ^\circ\mathrm{K}) = E_{g0} - \gamma_{300}\langle F_{300}^2\rangle\,, \tag{9}$$

where E_{g0} is the value of E_g in the undisturbed lattice, γ_{100} and γ_{300} are the FKC's at 100 and 300 °K, respectively, and $\langle F_{100}^2\rangle$ and $\langle F_{300}^2\rangle$ are the mean-square fields at these temperatures.

The measured shift in E_g,

$$\Delta E_g' = E_g(100\ ^\circ\mathrm{K}) - E_g(300\ ^\circ\mathrm{K}) \tag{10}$$

has to be written

$$\Delta E_g' = \gamma_{300}\langle F_{300}^2\rangle - \gamma_{100}\langle F_{100}^2\rangle\,. \tag{11}$$

From experimental data we know the values of γ_{100} (γ_{100} has been measured directly only in the cubic case[32]), γ_{300}, and $\Delta E_g'$. The theoretical value of $\langle F_{100}^2\rangle$ [Eq. (3)] has to be introduced in addition to the other known parameters in order to find the experimental magnitude of $\langle F_{300}^2\rangle$ from Eq. (11). The values of $(\langle F_{300}^2\rangle)^{1/2}$ as computed from Eq. (11) under the above assumptions appear in Table II and are called F_{expt}. The theoretical values of the F_{rms} field [Eq. (3)] of the LO phonons at 300 °K for both values of q_c are also tabulated there. One sees that the experimental values are well within the theoretical limits.

For the 4H and 2H structures only γ_{300} is known.[31] The tabulated experimental γ_{100} values are computed under the assumption that the ratio $\gamma_{100}/\gamma_{300}$ is the same as measured in the cubic crystal.

A similar procedure for the LA phonons will be used

$$\Delta E_g'' = E_g(50\ ^\circ\mathrm{K}) - E_g(100\ ^\circ\mathrm{K}) = E_g(50\ ^\circ\mathrm{K}) - \gamma_{100}\langle F_{100}^2\rangle\,. \tag{12}$$

TABLE II. ZnS; the Franz-Keldysh coefficients γ at $T = 100$ °K and $T = 300$ °K for three cystallization forms of ZnS; the root-mean-square electric field strength F_{rms} due to LO phonons at 300 °K, calculated by the Dow-Redfield theory [Eq. (3)] for both values of $q_c = \pi/2a$ and $q_c = \pi/a$; the electric field $F_{expt} = (\langle F_{300}^2\rangle)^{1/2}$ calculated from the experimental results [Eq. (11)] at 300 °K.

ZnS crystal	Polarization of light	$10^{12}\gamma$ (eV cm^2)/V^2 at 100 °K	$10^{12}\gamma$ (eV cm^2)/V^2 at 300 °K	$10^{-5}F_{rms}$ (V/cm) ($q_c = \pi/2a$)	$10^{-5}F_{rms}$ (V/cm) ($q_c = \pi/a$)	$10^{-5}F_{expt}$ (V/cm)
3C		4.92 [a]	1.72 [b]	2.03	5.75	3.90
4H	$\vec{E}\perp\vec{C}$	3.60 [c]	1.26 [b]	2.56	7.25	4.77
	$\vec{E}\parallel\vec{C}$	3.29 [c]	1.15 [b]	2.88	8.11	5.20
2H	$\vec{E}\perp\vec{C}$	2.06 [c]	0.72 [b]	3.50	9.99	6.34
	$\vec{E}\parallel\vec{C}$	1.72 [c]	0.60 [b]	4.54	12.80	7.62

[a] Reference 32.
[b] Reference 31.
[c] Not directly measured, but taken at same ratio to γ(300 °K) as measured in the cubic case.

The rms field evaluated by this method was found to be about 6×10^4 V/cm for the LA piezoelectric phonon in the 3*C* ZnS at 100 °K. A semitheoretical computation of these fields, using the published data both on the increment in the mean square displacement $\langle u^2\rangle$ due to the acoustic phonons[33] in the temperature region of 50–100 °K and the low-temperature piezoelectric constants[28] yields a similar result, of about 5×10^4 V/cm.

The possible contribution of the lattice dilatation to the gap energy was also considered. From known data on the pressure dependence of the edge[34] and the temperature dependence of the unit cell volume[35] it was found that the dilatation effect in 3*C* cubic ZnS is less than 10% of the measured $\Delta E_g'$. Therefore, we could disregard this part of $\Delta E_g'$ which also has the tendency to decrease the gap in ZnS.

From the tabulated results one can deduce that the functional dependence of the absorption edge on temperature as given by the Dow-Redfield theory, has been found to apply well in the case of ZnS crystals. On the other hand, accurate numerical comparisons between measured and computed values of the temperature shift of the absorption edge are more difficult. There the choice of the right polaron cutoff wave vector q_c, which is connected with the uniform-field approximation, is the major obstacle. With a choice of $\pi/a \geq q_c \geq \pi/2a$ the agreement between experiment and theory is good. More experimental data on additional ionic materials are necessary, before a final verdict on the general applicability of the Dow-Redfield theory can be made. So far the only available data are on some experiments made on CdS single crystals by Gutsche *et al.*[36] and by Dutton,[6] who measured the FKC and the temperature shift of the absorption edge, respectively. Table III sums up these data for CdS in a similar way as was done in Tables I and II for ZnS. Again a good fit is obtained between the theory and the experimental results.

SUMMARY

The strong temperature dependence of the exponential absorption edges in three ZnS structures, cubic, hexagonal, and 4*H* polytype, has been measured in the temperature range from 10 to 300 °K. Combining the Dow-Redfield theory of the phonon generated microfields and the Franz-Keldysh theory on the field induced shift of exponential absorption edges made it possible to explain the results quantitatively.

ACKNOWLEDGMENTS

We would like to thank Professor I. T. Steinberger and Dr. Z. H. Kalman for frequent discussions and valuable suggestions.

APPENDIX

ZnS crystals have a polar axis (which is the ⟨111⟩ axis in the 3*C* case and is the *c* axis in the birefringent ZnS crystals) so that these crystals will have piezoelectric properties.[39] The LA phonon along this polar axis will be accompanied by the highest piezoelectrical fields. As the Dow-Redfield theory demands quasiconstant fields over a distance commeasurable to the exciton radius, we have to consider that in the present case there has to be a similar critical cutoff wave vector q_c as in the LO case. Thus the short-wave zone boundary phonons should have no influence on the absorption edge.

The measured dispersion relation of the long-wave LA phonons follows the linear dependence of the wavelength frequency as based on the measured elastic constants of the materials.[40-43] We will investigate the temperature dependence of the expected piezoelectric fields. The mean square displacement of the ions depends on temperature as[44]

$$\langle u_k^2\rangle \propto \sum_{\vec{q},j} |\vec{e}(k,j,\vec{q})| \frac{\coth[\hbar\omega_j(\vec{q})/2kT]}{\omega_j(\vec{q})}, \qquad \text{(A1)}$$

TABLE III. Data for CdS, headings of columns as in Tables I and II, $h\omega_{LO}$ are the reported energy values of the longitudinal-optical phonon.

Polarization of light	$10^{12}\gamma$ (eV cm^2)/V^2 at 300 °K	μ^* (m_0)	ϵ_0	ϵ_∞	$h\omega_{LO}$ (meV)	$10^{-5}F_{rms}$ (V/cm) ($q_c=\pi/2a$)	$10^{-5}F_{rms}$ (V/cm) ($q_c=\pi/a$)	$10^{-5}F_{expt}$ (V/cm)
$\vec{E}\perp\vec{C}$	1.8 [a]	0.16 [b]	8.4 [c]	5.3 [c]	37.4 [c]	2.15	6.07	3.97
$\vec{E}\parallel\vec{C}$	1.1 [a]	0.20 [b]	8.9 [c]	5.4 [c]	36.9 [c]	2.98	8.43	5.90

[a] Reference 36.
[b] Reference 37.
[c] Reference 38.

where k is the index of the ion, $\omega_j(\vec{q})$ is the frequency of the normal mode with the wave vector $\vec{q}$ in the jth branch, and $\vec{e}\,(k,j,\vec{q})$ is the polarization vector of the corresponding displacement of the ion k.

For one single LA phonon in the ⟨111⟩ direction, the mean-square field is proportional to

$$\langle F^2\rangle \propto \mathfrak{D}^2\langle u^2\rangle/(\tfrac{1}{2}\lambda)^2\,, \tag{A2}$$

where λ is the wavelength associated with the phonon, here $\lambda^2 = 4\pi^2 v^2/\omega^2$, $\mathfrak{D}$ contains both the appropriate piezoelectric constant and the static dielectric constant, v is the sound velocity, and ω is the frequency of the phonon. For an assembly of LA phonons,

$$\sum_{\vec{q}} \langle F_{\mathrm{LA}}^2\rangle \propto \mathfrak{D}^2 \sum_{\vec{q}} \frac{g(\omega(\vec{q}))\coth[\hbar\omega(\vec{q})/2kT]}{\omega(\vec{q})(\frac{1}{2}\lambda)^2}\,, \tag{A3}$$

where $g(\omega(\vec{q}))$ is the phonon distribution function which for long-wave elastic vibrations is proportional:

$$g(\omega)\propto \omega^2\,. \tag{A4}$$

Combining (A3) and (A4), we obtain

$$\sum_{\vec{q}} \langle F_{\mathrm{LA}}^2\rangle \propto \sum_{\vec{q}} [\omega(\vec{q})]^3 \coth\left(\frac{\hbar\omega(\vec{q})}{2kT}\right). \tag{A5}$$

The highest mean-square fields will be due to the cutoff-frequency phonons, these will also be the most numerous so that their effect on the absorption edge will be predominant. As

$$\omega_c = 2\pi\nu/\lambda_c = 2vq_c\,, \tag{A6}$$

we can write

$$\langle F_{\mathrm{LA}}^2\rangle \propto q_c^3 \coth(\hbar\omega_c/2kT)\,, \tag{A7}$$

where the subscript c designates the cutoff values of the variables. In cubic ZnS, according to the results obtained from neutron scattering,[40-43] with $q_c/q_{\max} = 0.156$, we find[40] that $\omega_c \approx 2.15\times 10^{13}$ cps and $\hbar\omega_c \approx 14.2$ meV. This is to be compared with the zone boundary value of the LA phonon of[40] 23.1 meV and to the LA-phonon value as obtained from Raman scattering,[25] 13.6 meV. The symmetry of a Λ-axis phonon Raman scattering is the same as for a L-point phonon.[45] The similarity of the energies involved in both the Raman-scattering process and in the absorption edge shift is intriguing, the reason for the highest second-order scattering peak being at this frequency[26] might be due to the strong quasiconstant electric field accompanying this cutoff value piezoelectric Λ-axis LA phonon. A similar electric field enhancement of the first-order Raman scattering by the LO phonons in the zinc-blende-type semiconductors has been commented on before.[46] However, it is to be pointed out that other authors[47] have attributed these phonon values to a W_1 critical point at the Brillouin-zone boundary.

*Supported in part by the Central Research Fund of the Hebrew University.

[1]I. T. Steinberger, E. Alexander, Y. Brada, Z. H. Kalman, I. Kiflawi, and S. Mardix, J. Cryst. Growth 13/14, 285 (1972).
[2]O. Brafman and I. T. Steinberger, Phys. Rev. 143, 501 (1966).
[3]W. W. Piper, Phys. Rev. 92, 23 (1953).
[4]G. Shachar, Ph.D. thesis (The Hebrew University, Jerusalem, 1969) (unpublished).
[5]F. Urbach, Phys. Rev. 92, 1324 (1953); F. Moser and F. Urbach, *ibid.* 102, 1519 (1956).
[6]D. Dutton, Phys. Rev. 112, 785 (1958).
[7]H. Mahr, Phys. Rev. 125, 1510 (1962); 132, 1880 (1963).
[8]J. R. Dixon and J. M. Ellis, Phys. Rev. 123, 1560 (1961).
[9]D. Redfield and M. A. Afromowitz, Appl. Phys. Lett. 11, 138 (1967).
[10]F. Möglich, N. Riehl, and R. Rompe, Z. Tech. Phys. 21, 6, 128 (1940).
[11]A. Radkowsky, Phys. Rev. 73, 749 (1948).
[12]H. Y. Fan, Phys. Rev. 82, 900 (1951).
[13]G. Hohler, Ann. Phys. (Leipz.) 4, 371 (1949).
[14]W. W. Piper, D. T. F. Marple, and P. D. Johnson, Phys. Rev. 110, 323 (1958).
[15]W. W. Piper, P. D. Johnson, and D. T. F. Marple, J. Phys. Chem. Solids, 8, 457 (1959).
[16]Y. F. Tsay, S. S. Mitra, and J. F. Vetelino, J. Phys. Chem. Solids 34, 2167 (1973).
[17]J. D. Dow and D. Redfield, Phys. Rev. B 5, 594 (1972).
[18]D. Redfield, Phys. Rev. 130, 916 (1963); Trans. N. Y. Acad. Sci. 26, 590 (1964).
[19]D. L. Dexter, Phys. Rev. Lett. 19, 1383 (1967).
[20]H. Fröhlich, U. Pelzer, and S. Zienau, Philos. Mag. 41, 221 (1950).
[21]W. Franz, Z. Naturforsch. A 13, 484 (1958).
[22]Y. Brada and B. G. Yacobi, in *Proceedings of the Twelfth International Conference on the Physics of Semiconductors*, edited by M. H. Pilkuhn (Teubner, Stuttgart, 1974), p. 1212.
[23]C. Z. Van Doorn, Physica (Utr.) 20, 1155 (1954).
[24]O. Brafman and S. S. Mitra, Phys. Rev. 171, 931 (1968).
[25]W. G. Nilsen, Phys. Rev. 182, 838 (1969).
[26]W. G. Nilsen, in *Light Scattering Spectra of Solids*, edited by G. B. Wright (Springer, Berlin, Heidelberg, New York, 1969), p. 129.
[27]J. Schneider and R. D. Kirby, Phys. Rev. B 6, 1290 (1972).
[28]D. Berlincourt, H. Jaffe, and L. R. Shiozawa, Phys. Rev. 129, 1009 (1963).
[29]I. B. Kobyakov and G. S. Pado, Fiz. Tverd. Tela. 9, 2173 (1967) [Sov. Phys.—Solid State 9, 1707 (1968)].
[30]R. H. Lyddane, R. G. Sachs, and E. Teller, Phys. Rev. 59, 673 (1941).
[31]B. G. Yacobi and Y. Brada, Phys. Rev. B 10, 665 (1974).

[32]B. G. Yacobi, Ph.D. thesis (The Hebrew University, Jerusalem, 1974) (unpublished).
[33]J. F. Vetelino, S. P. Gaur, and S. S. Mitra, Phys. Rev. B 5, 2360 (1972).
[34]A. L. Edwards, T. E. Slykhouse, and H. G. Drickamer, J. Phys. Chem. Solids 11, 140 (1959).
[35]H. Von Adenstedt, Ann. Phys. (Leipz.) 26, 69 (1936).
[36]E. Gutsche and H. Lange, Phys. Status Solidi 4, K21 (1964); 13, K131 (1966).
[37]J. J. Hopfield and D. G. Thomas, Phys. Rev. 122, 35 (1961).
[38]M. Balkanski, in *II-VI Semiconducting Compounds*, edited by D. Thomas (Benjamin, New York, 1967), p. 1007.
[39]W. G. Cady, *Piezoelectricity* (Dover, New York, 1964).
[40]L. A. Feldkamp, G. Venkataraman, and J. S. King, Solid State Commun. 7, 1571 (1969).
[41]J. F. Vetelino, S. S. Mitra, and O. Brafman, Solid State Commun. 7, 1809 (1969).
[42]J. Bergsma, Phys. Lett. A 32, 324 (1970).
[43]N. Vagelatos, D. Wehe, and J. S. King, J. Chem. Phys. 60, 3613 (1974).
[44]A. A. Maradudin, E. W. Montroll, and G. H. Weiss, *Solid State Physics*, edited by F. Seitz and D. Turnbull (Academic, New York, 1963), Suppl. 3.
[45]R. H. Parmenter, Phys. Rev. 100, 73 (1955).
[46]H. Poulet, Ann. Phys. (Paris) 10, 908 (1955).
[47]D. N. Talwar and Bal K. Agrawal, Phys. Status Solidi B 64, 71 (1974).